

Coherent Potential Approximation for ‘d - wave’ Superconductivity in Disordered Systems.

A.M. Martin

Département de Physique Théorique, Université de Genève, 1211 Genève 4, Switzerland.

G. Litak

Department of Mechanics, Technical University of Lublin, Poland.

B.L. Györfy, J.F. Annett

*H.H. Wills Physics Laboratory, University of Bristol, Royal Fort, Tyndall Avenue, Bristol BS8
1TL, UK.*

K.I. Wysokiński.

Institute of Physics, Maria Curie-Skłodowska University, Lublin, Poland.

(October 21, 2018)

Abstract

A Coherent Potential Approximation is developed for s -wave and d -wave superconductivity in disordered systems. We show that the CPA formalism reproduces the standard pair-breaking formula, the self-consistent Born Approximation and the self-consistent T -matrix approximation in the appropriate limits. We implement the theory and compute T_c for s -wave and d -wave pairing using an attractive nearest neighbor Hubbard model featuring both binary alloy disorder and a uniform distribution of scattering site potentials. We determine the density of states and examine its consequences for low temperature heat capacity. We find that our results are in qualitative agreement

with measurements on Zn doped YBCO superconductors.

Pacs. 74.62.Dh, 74.20-z

I. INTRODUCTION

A treatment of disorder is an essential part of the theory of superconductivity. After all, one must explain why impurity scattering does not cause resistance. Thus it is natural that as evidence for novel superconducting states multiplies the foundations of the subject, due mainly to Anderson¹ and Abrikosov and Gorkov^{2,3}, are being re-examined. The experiments which stimulate most strongly the current revival of interest in the problem are those on the high temperature superconductors⁴, which are now universally regarded as ‘*d*-wave superconductors’⁵, and those involving some of the heavy fermion systems which display signs of ‘*p*-wave’ pairing⁶. In what follows we wish to contribute to the theoretical discussion⁷⁻¹⁴ of the issues raised by these very interesting developments.

The case of classic, ‘*s*-wave’, superconductors is by now well understood. If the perturbation does not break time reversal symmetry and the coherence length is sufficiently long, so that the pairing potential Δ does not fluctuate, the Anderson Theorem¹ guarantees that there is an absolute gap in the quasi-particle spectrum and the main effect of disorder is that the density of normal states in the gap equation is replaced by its average over configurations¹⁵. On the other hand if the perturbation breaks time reversal invariance, as is the case with paramagnetic impurities, the effect is more dramatic. For instance, the transition temperature T_c is reduced from its clean limit value T_{c0} , according to the well known pair-breaking formula:

$$\ln\left(\frac{T_c}{T_{c0}}\right) = \psi\left(\frac{1}{2}\right) - \psi\left(\frac{1}{2} + \rho_c\right) \quad (1)$$

where $\psi(x)$ is the digamma function and $\rho_c = (2\pi\tau T_c)^{-1}$ is a measure of the strength of the scattering and τ^{-1} is the scattering rate^{2,7}.

By contrast in the case of superconductors whose Cooper pairs are of exotic ‘*p*-wave’ or ‘*d*-wave’ character even simple potential scattering, which does not break time reversal symmetry, causes pair breaking⁷. This fact was noted already in the early contributions to the field¹⁷, but has become a subject of intense scrutiny only recently⁷⁻¹⁴. Of particular

interest are two dimensional models featuring ‘ d -wave’ pairing as these may be relevant to experiments on high T_c superconductors. Notably, for cuprates many experiments have explored the variation of T_c , the density of states and other properties as a function of Ni and Zn substitutions on the copper sites^{16,18-24} or irradiation damage²⁵⁻²⁷. Although a wide variety of theoretical ideas²⁸⁻³² and methods³³⁻³⁸ have been applied to interpret the experiments a comprehensive picture of the role of disorder is far from complete. On a more formal level, an intriguing problem arises from the observation of Gorkov and Kalugin¹⁰ that the scattering in models where the order parameter has a line of zeros on the Fermi surface is highly singular and this may be a manifestation of interesting new physics. Indeed in 2-d, Nersesyan *et al.*¹⁴ predict that the quasi particle density of states $N(E)$ approaches zero, even in the disordered state, as power law, $\sim |E|^\alpha$, with positive exponent α , instead of going to a finite value

$$N(0) \sim \frac{1}{\gamma} e^{-\frac{1}{\gamma}} \quad (2)$$

where γ measures strength of the interaction, as was found by Gorkov and Kalugin¹⁰. Another interesting and controversial issue is the relative importance of the self-consistent Born approximation (SCBA) and resonant scattering in the unitarity limit^{11,12}. Our aim here is to explore the subject systematically on the bases of explicit calculations, albeit for a simple, extended Hubbard model with attractive interactions and site diagonal randomness only.

In short we will examine the problem of disordered unconventional superconductors making use of the coherent potential approximation (CPA). The CPA is the most reliable approximation developed for the theory of electronic structure of random metallic alloys in the normal state^{39,40}. Notably it has been shown to be exact in both the weak and the strong scattering limits, and applicable to systems with low as well as high concentration of impurities. Significantly, the CPA reduces to the self-consistent Born approximation (SCBA) for weak scattering impurities, and agrees with the self-consistent T-matrix approximation (SCTA) results for strongly scattering impurities of low concentrations. Indeed it remains a good approximation in the unitarity limit of resonant scattering^{11,12}. Finally, on account of

the fact that it becomes exact as the number of nearest neighbors goes to infinity, the CPA is often referred to as a mean field theory of disorder⁴¹.

Given these desirable features it is clearly worthwhile to explore the consequences of the CPA for disordered superconductors. For the case of conventional s -wave pairing this has already been done, generating many useful results^{42,43}. Apart from our earlier brief report⁴⁴ and the limited discussion in Ref. 45, the case of superconductors with Cooper pairs of d symmetry will be treated here, within CPA, for the first time.

We will describe fully our numerical method, demonstrate that in various limits our formalism reproduces many of the well known results for disordered superconductors, and examine in detail the phase diagram of the local and non-local attractive two-dimensional Hubbard models. In particular we study the variations of T_c with impurity scattering strength and with impurity concentration for the case of local s -wave pairing as well as non-local (extended) s -wave and d -wave pairing. We also contrast the cases for a binary alloy, A-B type, disorder with the case of uniformly distributed scattering potentials on each site. Finally, we investigate the DOS, $N(E)$, at low energies and its consequences for measurements of the specific heat, comparing our results with those of Kalugin and Gorkov¹⁰, Eq. 2, and of Nereseyan, Tsvelik and Wenger¹⁴.

II. INCORPORATING THE CPA INTO THE BOGOLIUBOV DE GENNES EQUATION

Our starting point is the single band Hubbard model with an attractive extended interaction which is described by the following Hamiltonian

$$H = \sum_{ij\sigma} t_{ij} c_{i\sigma}^\dagger c_{j\sigma} + \frac{1}{2} \sum_{ij} U_{ij} \hat{n}_i \hat{n}_j - \sum_i (\mu - \varepsilon_i) \hat{n}_i \quad (3)$$

where $c_{i\sigma}^\dagger$ and $c_{i\sigma}$ are, respectively, the usual creation and annihilation operators for electrons on site i with spin σ , and the local charge operator is $\hat{n}_i = \hat{n}_{i\uparrow} + \hat{n}_{i\downarrow}$ with $\hat{n}_{i\sigma} = c_{i\sigma}^\dagger c_{i\sigma}$. The chemical potential is μ , t_{ij} are the hopping integrals (for $i \neq j$) and ε_i is the local site energy.

The interaction term, $U - ij$, can be either be a local attractive interaction ($U_{ii} < 0$) giving rise to s -wave pairing, or a non-local attractive interaction ($U_{ij} < 0$ for $i \neq j$) giving rise to d -wave or extended s -wave pairing. Disorder is introduced into the problem by allowing the site energies, ϵ_i , to vary randomly from site to site.

Starting from Eq. (3) we apply the Hartree-Fock-Gorkov^{46,47} approximation, which results in the following Bogoliubov de Gennes equation:

$$\sum_l \begin{pmatrix} (\omega_n - \epsilon_i + \mu)\delta_{il} + t_{il} & \Delta_{ij} \\ \Delta_{ij}^* & (\omega_n + \epsilon_i - \mu)\delta_{il} - t_{il} \end{pmatrix} \begin{pmatrix} G_{11}(l, j; \omega_n) & G_{12}(l, j; \omega_n) \\ G_{21}(l, j; \omega_n) & G_{22}(l, j; \omega_n) \end{pmatrix} = \delta_{ij} \begin{pmatrix} 1 & 0 \\ 0 & 1 \end{pmatrix}, \quad (4)$$

for the Greens function matrix $G(i, j; \omega_n)$ at the Matsubara frequency, $\hbar\omega_n = (2n+1)\pi k_B T$. For computational convenience we shall take the hopping integral t_{ij} to be non zero only when the sites i and j are nearest neighbors. The mean field pairing potential Δ_{ij} can either be local ($i = j$) or nearest neighbor non-local, see Fig. 1, and couples particle and hole amplitudes between sites i and j . Of course, the above equations are completed by the self-consistency condition that

$$\Delta_{ij} = |U_{ij}| \frac{1}{\beta} \sum_n e^{i\omega_n \eta} G_{12}(i, j; \omega_n), \quad (5)$$

where η is a positive infinitesimal. To simplify matters we have assumed that the normal Hartree and exchange terms can be absorbed into the definitions of the chemical potential, μ , or the hopping integrals t_{ij} . As usual, Eqs. (4) and (5) are to be solved subject to the requirement on the chemical potential that

$$n = \frac{2}{\beta} \sum_n e^{i\omega_n \eta} G_{11}(i, i; \omega_n), \quad (6)$$

where n is the average number of electrons per unit cell. Clearly, the Greens function matrix $\mathbf{G}(i, j; \omega_n)$ determined by the above equations depends on the set of site energies $\{\epsilon_i\}$. Our task is to find the configurationally averaged Greens function matrix $\langle \mathbf{G}(i, j; \omega_n) \rangle$. Evidently, this is made much easier if we assume that the pairing potential does not fluctuate from configuration to configuration. As was argued by Gyorffy *et al.*¹⁵ this is a good approximation when the T=0 coherence length ξ_0 is large. Thus our results will have to be

treated with appropriate care when applied to superconductors with short coherence length such as superconducting cuprates.

Let us now proceed to deploy the CPA strategy for calculating the averaged Greens function matrix $\langle \mathbf{G}(i, j; \omega_n) \rangle$ subject to the self consistency conditions:

$$\bar{\Delta}_{ij} = |U_{ij}| \frac{1}{\beta} \sum_n e^{i\omega_n \eta} \langle G_{12}(i, j; \omega_n) \rangle, \quad (7)$$

$$\bar{n} = \frac{2}{\beta} \sum_n e^{i\omega_n \eta} \langle G_{11}(i, i; \omega_n) \rangle. \quad (8)$$

The first move in deriving the fundamental equations of the coherent potential approximation is to define a coherent medium Greens function matrix $\mathbf{G}^c(i, j; \omega_n)$ by

$$\sum_l \begin{pmatrix} (i\omega_n + \mu - \Sigma_{11}(i\omega_n))\delta_{il} + t_{il} & \bar{\Delta}_{il} \\ \bar{\Delta}_{il}^* & (i\omega_n - \mu - \Sigma_{22}(i\omega_n))\delta_{il} - t_{il} \end{pmatrix} \mathbf{G}^c(l, j; \omega_n) = \delta_{ij} \begin{pmatrix} 1 & 0 \\ 0 & 1 \end{pmatrix}. \quad (9)$$

As will be clear latter $\mathbf{G}^c(i, j; \omega_n) = \langle \mathbf{G}(i, j; \omega_n) \rangle$ and hence $\Sigma_{11}(i\omega_n)$ and $\Sigma_{22}(i\omega_n)$ are the diagonal components of the usual self-energy. Note that we did not introduce any off diagonal self-energies such as $\Sigma_{12}(i\omega_n)$ and $\Sigma_{21}(i\omega_n)$ because for the single site perturbations of our model they are zero. The next step is to consider the scattering of the quasi-particles, propagating according to $\mathbf{G}^c(i, j; \omega_n)$ by the defects described by the potentials:

$$\mathbf{V}^l(i\omega_n) = \begin{pmatrix} \varepsilon^l & 0 \\ 0 & -\varepsilon^l \end{pmatrix} - \begin{pmatrix} \Sigma_{11}(i\omega_n) & 0 \\ 0 & \Sigma_{22}(i\omega_n) \end{pmatrix}, \quad (10)$$

where l labels one of the m different site energies we wish to consider.

In a straightforward application of the CPA principles,⁴⁰ $\Sigma(i\omega_n)$ and therefore $\mathbf{G}^c(i, j; \omega_n)$ is determined by the condition that these defects do not scatter on the average *i.e.*

$$\sum_{l=1}^m c_l \mathbf{T}^l(i\omega_n) = 0 \quad (11)$$

where

$$\mathbf{T}^l(i\omega_n) = \mathbf{V}^l(i\omega_n) \left[\mathbf{1} - \mathbf{G}^c(i, j; \omega_n) \mathbf{V}^l \right]^{-1} \quad (12)$$

and

$$\sum_{l=1}^m c_l = 1. \quad (13)$$

From Eqs. (11,12) it is now possible, in conjunction with equations (7-9), to calculate $\Sigma(i\omega_n)$ and $\mathbf{G}^c(i, j; i\omega_n)$. The numerical methodology for calculating $\mathbf{G}^c(i, j; i\omega_n)$ and $\Sigma(i\omega_n)$ closely follows that in Ref. 48 and is outlined in Appendix A.

A number of recent studies of superconductors with unconventional pairing suggest that the consequences of disorder depend sensitively on the models used to describe the randomness.^{49,50} Thus we are going to investigate two different models. The first corresponds to binary alloy disorder, where $m = 2$. Namely we consider two *types* of sites with site energies ε_1 and ε_2 and concentrations of c and $1 - c$ respectively. The second model is described by a uniform distribution of site energies. Here we shall have in mind the limit where $m \rightarrow \infty$ with $\varepsilon_l \in [-\frac{\delta}{2}, \frac{\delta}{2}]$. Consequently in Eq. (11) the sum \sum_l becomes the integral $\frac{1}{\delta} \int d\varepsilon_l$.

In the bimodal case, where $m = 2$, we can simplify Eq. (11) to find

$$\Sigma_{11}(i\omega_n) = (2c - 1)\frac{\delta}{2} - \left(\frac{\delta}{2} - \Sigma_{11}(i\omega_n)\right)G_{11}^c(i\omega_n)\left(-\frac{\delta}{2} - \Sigma_{11}(i\omega_n)\right) \quad (14)$$

where $|\varepsilon_1 - \varepsilon_2| = \delta$.

In the second, uniform distribution, case we transform the sum in equation (11) into an integral so that

$$\frac{1}{\delta} \int_{-\frac{\delta}{2}}^{\frac{\delta}{2}} T^l(i\omega_n) d\varepsilon_l = 0. \quad (15)$$

After some straightforward algebra this leads to

$$\Sigma_{11}(i\omega_n) = -\frac{1}{G_{11}^c(i\omega_n)} + \frac{\delta}{2} \frac{1}{\tanh\left(\frac{\delta G_{11}^c(i\omega_n)}{2}\right)}. \quad (16)$$

Thus our CPA calculations will consist of solving numerically either Eq. (14) for the bimodal distribution of the site energies, or Eq. (16) for the case of uniform distribution, to determine the self-energies $\Sigma_{11}(i\omega_n)$ and $\Sigma_{22}(i\omega_n)$.

III. PAIR BREAKING FORMULA IN CPA

We now relate the CPA formulae derived above to the usual results of disordered superconductors, corresponding to the well known pair breaking formula Eq. (1). As is well known⁷ the pair breaking formula was first derived for magnetic impurities in s -wave superconductors² but it also applies in many other interesting circumstances such as our present concern, namely the case of non-magnetic impurities in d -wave superconductors¹⁷.

To derive it within the CPA let us start with the gap equation

$$\Delta_{\vec{k}} = \frac{1}{N} \sum_{\vec{q}} U_{\vec{k}-\vec{q}} \frac{1}{\beta} \sum_{\omega_n} G_{12}^c(\vec{q}; \omega_n) e^{i\omega_n \delta}. \quad (17)$$

As a motivation for our argument we recall the method of Abrikosov and Gorkov² for solving the gap equation at T_c for a clean superconductor. In that case, to find T_c we linearize the analogue of Eq.(17) by approximating the off diagonal Greens function G_{12}^c as follows:

$$G_{12}^c(\vec{q}; \omega_n) \cong \frac{\Delta_{\vec{q}}}{(i\omega_n - \xi_{\vec{q}})(i\omega_n + \xi_{\vec{q}})} \quad (18)$$

where $\xi_{\vec{q}} = \varepsilon_{\vec{q}} + \mu$, and for our tight binding model with a square lattice $\varepsilon_{\vec{q}} = -2t(\cos(q_x) + \cos(q_y))$. Then, we note that the kernel of the linear integral equation for $\Delta(\vec{k})$ is a four term degenerate kernel:

$$U(\vec{k} - \vec{q}) = |U|(\eta_{\vec{k}}\eta_{\vec{q}} + \gamma_{\vec{k}}\gamma_{\vec{q}} + 2 \sin k_x \sin q_x + 2 \sin k_y \sin q_y), \quad (19)$$

where $\eta_{\vec{k}} = 2(\cos(k_x) - \cos(k_y))$ and $\gamma_{\vec{k}} = 2(\cos(k_x) + \cos(k_y))$. Consequently, the general $\Delta(\vec{k})$ will be a linear superposition of $\eta_{\vec{k}}$, $\gamma_{\vec{k}}$, $\sin k_x$ and $\sin k_y$. However, when the internal symmetry of the singlet Cooper pair is pure d -wave we may take $\Delta(\vec{k})$ to be of the form

$$\Delta_{\vec{k}} = \Delta_{\eta} \eta_{\vec{k}}. \quad (20)$$

Then the condition for non-zero order parameter becomes

$$1 = \frac{|U|}{N} \sum_{\vec{q}} \frac{\eta_{\vec{q}}^2}{4} T_{c0} \sum_{\omega_n} \frac{1}{\omega_n^2 - \xi_{\vec{q}}^2}. \quad (21)$$

Let us now define a d -wave weighted density of states

$$N_d(E) = \frac{1}{N} \sum_{\vec{q}} \frac{\eta_{\vec{q}}^2}{4} \delta(E - \xi_{\vec{q}}) \quad (22)$$

and write the above condition, which determines the transition temperature T_{c0} , as

$$1 = |U| \int_{-\infty}^{\infty} dE N_d(E) T_{c0} \sum_{\omega_n > 0} \frac{2}{\omega_n^2 + E^2}, \quad (23)$$

where $\omega_n = \pi T_{c0}(2n + 1)$. In the above equation the integral and the sum are divergent, so we need to introduce a cut-off, ω_n^c . In the usual way we assume the density of states $N_d(E)$ is slowly varying up to the cut off energy, so we will make the approximation $N_d(E) = N_d(0)$.

Then, considering that

$$N_d(0) \int_{-\infty}^{\infty} dE \frac{1}{\omega_n^2 + E^2} = \pi N_d(0) \frac{1}{\omega_n} \quad (24)$$

we can write

$$1 = |U| N_d(0) 2\pi T_{c0} \sum_{\omega_n > 0}^{\omega_n^c} \frac{1}{\omega_n}. \quad (25)$$

and hence rewrite Eq. (23) as

$$\frac{1}{|U| N_d(0)} = \psi\left(\frac{1}{2} + \frac{\omega_n^c}{2\pi T_{c0}}\right) - \psi\left(\frac{1}{2}\right) \approx \ln\left(\gamma \frac{\omega_n^c}{2\pi T_{c0}}\right). \quad (26)$$

This is the BCS result for the superconducting transition temperature in the case of d -wave pairing⁴⁶. It differs from the conventional result only in that the d -projected density of states $N_d(0)$ has replaced the usual full density of states $N(0)$.

Let us now return to disordered superconductors and examine how the above well known argument is modified when the randomness is dealt with within the CPA. Using Eq. (9) it can be easily seen that instead of Eq. (18) we should use

$$G_{12}^c(\vec{q}; \omega_n) = \frac{\Delta_{\vec{q}}}{(i\omega_n - \xi_{\vec{q}} - \Sigma_{11}(i\omega_n))(i\omega_n + \xi_{\vec{q}} - \Sigma_{22}(i\omega_n))}. \quad (27)$$

to linearize Eq. (17) at T_c . Thus, noting that

$$\Sigma_{22}(i\omega_n) = -\Sigma_{11}(-i\omega_n) \quad (28)$$

the condition which determines T_c can be written as

$$1 = |U| \int_{-\infty}^{\infty} dE N_d(E) T_c \sum_{\omega_n > 0} \frac{2}{(\omega_n - E - \Sigma_{11}(i\omega_n))(\omega_n + E + \Sigma_{11}(-i\omega_n))}. \quad (29)$$

Now, at this point we need to know the form of $\Sigma_{11}(i\omega_n)$ to progress any further. As a first approximation we assume that the most important component to the self-energy is the component at the Fermi energy $E = E_F = \mu$. Later on we will test the accuracy of this approximation by examining our numerical results for $\Sigma_{11}(i\omega_n)$. For now, however, let us proceed by taking

$$\Sigma_{11}(i\omega_n) = i|\Sigma_0| \text{sgn}(\omega_n). \quad (30)$$

Evidently this leads to

$$1 = |U| \int_{-\infty}^{\infty} dE N_d(E) T_c \sum_{\omega_n > 0} \frac{2}{(i\omega_n - E + i|\Sigma_0| \text{sgn}(\omega_n))(i\omega_n + E + i|\Sigma_0| \text{sgn}(\omega_n))}. \quad (31)$$

Again taking $N_d(E)$ outside of the integration as $N_d(0)$ and performing the integration over E we find

$$1 = |U| N_d(0) 2\pi T_c \sum_{\omega_n > 0}^{\omega_n^c} \frac{1}{\omega_n + |\Sigma_0|} \quad (32)$$

where again the sum is cut off, as in the clean limit, by ω_n^c . If we now add and subtract the terms corresponding to $\Sigma_0 = 0$ (the clean case) we find

$$\frac{1}{|U| N_d(0)} = 2\pi T_c \sum_{\omega_n > 0}^{\omega_n^c} \frac{1}{\omega_n} + 2\pi T_c \sum_{\omega_n > 0}^{\omega_n^c} \left(\frac{1}{\omega_n + |\Sigma_0|} - \frac{1}{\omega_n} \right). \quad (33)$$

Clearly the term $\frac{1}{|U| N_d(0)}$ on the LHS of Eq. (33) can be replaced by $\ln\left(\gamma \frac{\omega_n^c}{2\pi T_{c0}}\right)$ on account of Eq. (26). With the same accuracy the first sum on the RHS of equation (33) equals $\ln\left(\gamma \frac{\omega_n^c}{2\pi T_c}\right)$ and the second sum is convergent. Hence the cutoff ω_n^c can be extended to infinity. As has been noted frequently before this infinite sum can be readily performed² and we find

$$\ln\left(\frac{T_c}{T_{c0}}\right) = \psi\left(\frac{1}{2}\right) - \psi\left(\frac{1}{2} + \rho_c\right). \quad (34)$$

where

$$\rho_c = \frac{|\Sigma_0|}{2\pi T_c}. \quad (35)$$

Eqs. (34) and (35) are the central results of this section. Reassuringly, whilst equation (34) is the standard pair-breaking formula,⁷ Eq. (35) is a very natural, but novel, CPA expression for the pair breaking parameter ρ_c . Recall that our derivation of the above result from CPA involved the approximation: $\Sigma_{11}(i\omega_n) \cong \Sigma_0$. To test the validity of this approximation we wish to compare exact CPA numerical results with the predictions of the analytical expression: Eqs. (34) and (35). Using numerical solutions of the CPA equation, to be discussed later, Fig. 2 plots the pair breaking strength ρ_c vs. δ/t , the disorder strength for the binary alloy type disorder. To find pair breaking parameter ρ_c we calculate T_c for each disorder strength, δ/t , and inverted Eq. (34) to obtain an effective ρ_c . The exact CPA ρ_c can then be compared to the solid line in Fig. 2 where we have taken our numerically calculated values for Σ_0 and directly calculated ρ_c , via Eq. (35). Finally the dashed line in Fig. 2 corresponds to ρ_c obtained using the Self-Consistent Born Approximation (SCBA). Evidently, the self energy at the Fermi energy, $E - \mu = 0$, Σ_0 , gives a good description of the pair breaking parameter ρ_c via Eq. (34). Also it is clear that, as expected, the Self-consistent Born Approximation $\Sigma_0 \equiv \frac{\hbar}{\tau} = \pi\delta^2 N(0)$ only works well in the weak scattering limit.

IV. ANALYTICAL FEATURES AND PREDICTIONS OF CPA EQUATIONS

In this section we examine various analytically accessible limits of the CPA formalism described above. Firstly, we demonstrate that Anderson's theorem is obeyed for s -wave superconductors and the CPA equations are consistent with the results of Abrikosov and Gorkov². Secondly we show that for d -wave superconductors the quasi particle density of states at the Fermi energy, $N(0)$, is non-zero in the presence of non magnetic disorder scattering and is consistent with the Gorkov-Kalugin formula, Eq. (2).

A. The Anderson's Theorem in the Coherent Potential Approximation

Formally, the CPA Eqs. (11) ,(12) can be written in terms of renormalized Matsubara frequencies, $\tilde{\omega}_n$, pairing parameter, $\tilde{\Delta}_{\vec{k}}$, and particle energies $\tilde{\xi}_{\vec{k}}$. This quantities are defined as follows

$$\tilde{\omega}_n = \omega_n \left(1 - \frac{i \text{Im} \Sigma_{11}(i\omega_n)}{\omega_n} \right) \quad (36)$$

$$\tilde{\Delta}_{\vec{k}} = \bar{\Delta}_{\vec{k}} \quad (37)$$

$$\tilde{\xi}_{\vec{k}} = \xi_{\vec{k}} - \mu - \text{Re} \Sigma_{11}(i\omega_n), \quad (38)$$

consequently

$$G_{11}(i\omega_n) = \frac{1}{N} \sum_{\vec{k}} \frac{i\tilde{\omega}_n + \tilde{\xi}_{\vec{k}}}{(i\tilde{\omega}_n)^2 - \tilde{\xi}_{\vec{k}}^2 - \tilde{\Delta}_{\vec{k}}^2} \quad (39)$$

and for the alloy type disorder with $c = 0.5$ and $\varepsilon = \pm\delta/2$, the self energy $\Sigma_{11}(i\omega_n)$ which renormalizes ω_n , $\Delta_{\vec{k}}$ and $\xi_{\vec{k}}$, and is defined by Eq. (14) can be written as

$$\Sigma_{11}(i\omega_n) = \frac{\frac{\delta^2}{4} G_{11}^c(i\omega_n)}{1 + G_{11}^c(i\omega_n) \Sigma_{11}(i\omega_n)} \quad (40)$$

The alternative expression for $\Sigma_{11}(i\omega_n)$ in the case of a uniform distribution of local potentials, $-\delta/2 < \varepsilon^l < \delta/2$ is given in Eq. (16).

Note that in the case of a non isotropic, d -wave gap, $\Delta_{\vec{k}}$, is not renormalized if the disorder is diagonal both in site and Nambu space. This is different from the case of local s -wave pairing where, as can be readily shown, $\Delta_{\vec{k}}$ is renormalized by the same factor as $\tilde{\omega}_n$ in Eq. (36). Thus for conventional superconductors, in contradiction to Eqs. (36) - (39), we find that the CPA yields

$$\frac{\tilde{\omega}_n}{\omega_n} = \frac{\tilde{\Delta}}{\Delta}, \quad (41)$$

in agreement with Born approximation or Abrikosov-Gorkov theory². As is widely appreciated^{2,15} the above equation implies the Anderson's Theorem in s -wave superconductors. By contrast in the d -wave case represented by Eqs. (36), Eq.(41) does not hold and hence there is no Anderson theorem.

Finally in concluding this section we would like to stress that Eqs. (36) - (40) represent strictly pure d -wave result. Even if we stick to the singlet case a more general solution of the CPA equation will imply a renormalization of $\Delta_{\vec{k}}$ to $\tilde{\Delta}_{\vec{k}}$. A good example of such situation is a case where the symmetry of $\Delta_{\vec{k}}$ is of extended s -wave symmetry $s^* \propto (\cos(k_x) + \cos(k_y))$ type. We shall encounter this interesting circumstance later on in this paper.

B. Density of States $N(0)$ in d -wave superconductors

Moving on and returning to the d -wave case, we observe that the form of Eqs. (36) - (40) are the same as were found by Larkin.¹⁷ Thus again the CPA reproduces the expected general form of the gap and frequency renormalizations, but with an improved description of the disorder. The most prominent feature of a conventional superconductor is vanishing of the quasi particle density of states $N(\varepsilon)$ for energies ε measured from the Fermi energy ε_F , less than Δ . In the case of clean, d -wave superconductors the line of zeros of $\Delta(\vec{k})$ on the Fermi surface leads to finite $N(\varepsilon)$ for all ε except $\varepsilon = 0$. In fact as is well known⁷ $N(\varepsilon)$ approaches zero linearly in ε . In the present section we shall investigate what happens to $N(\varepsilon)$ in the presence of disorder.

As it turns out for a given gap parameter $\bar{\Delta}_k = \Delta\eta_k$ and in the limit of small disorder $\delta \rightarrow 0$ the CPA equations can be solved analytically. To affect the solution note that in Eq. (39) the major part of the summation is coming from the four singular points in the Brillouin zone where the denominator vanishes:

$$i\tilde{\omega}_n^2 - \tilde{\xi}_k^2 - \tilde{\Delta}_k^2 = 0 \quad (42)$$

Linearizing around these points and performing the summation over k analytically, we find that

$$G_{11}^c(0) = \frac{i\text{Im}\Sigma_{11}(0)}{2\alpha} \ln \left| \frac{(4\Delta)^2 + (\text{Im}\Sigma_{11}(0))^2}{(\text{Im}\Sigma_{11}(0))^2} \right| \quad (43)$$

where $\alpha = 2t\Delta\pi$. Clearly in the limit $|\text{Im}\Sigma_{11}(0)| \ll 4\Delta$ this leads to

$$G_{11}^c(0) \approx \frac{i\text{Im}\Sigma_{11}(0)}{\alpha} \ln \left| \frac{4\Delta}{\text{Im}\Sigma_{11}(0)} \right|. \quad (44)$$

Moreover, when $\Sigma_{11}(i\omega_n)$ is small compared to the band width we can rewrite Eq. (40), using the Self-Consistent Born Approximation as

$$\Sigma_{11}(i\omega_n) = \frac{\delta^2}{4} G_{11}^c(i\omega_n). \quad (45)$$

On substituting this result into Eq. (44) the later becomes an equation for $G_{11}^c(0)$ which determines the density of quasi particle state $N(0)$ via the formula $N(0) = \frac{1}{\pi} G_{11}^c(i\omega_n = 0)$.

Indeed we find

$$N(0) \approx \frac{4\Delta t}{\pi\delta^2} e^{-\frac{8\pi\Delta t}{\delta^2}} \quad (46)$$

and

$$-\text{Im}\Sigma_{11}(0) \approx 4\Delta t e^{-\frac{8\pi\Delta t}{\delta^2}}. \quad (47)$$

These formulae agree with the results of Kalugin and Gorkov¹⁰ and Haas *et al.*²⁸ and have been verified numerically. For example Figs. 3 and 4 compare $N(0)$ as calculated from Eq. (46) and calculated using completely self-consistent CPA. As one can see there is good agreement between the two results and thus we conclude that at $\varepsilon = 0$ the density of states, in CPA, becomes finite when an arbitrary small amount of disorder is introduced. However, one should note that at very low levels of disorder our numerical results tend to a constant, whereas the analytical results tend to zero, this comes from the small complex component we have added to the energy to enable us to evaluate the Greens function. For a more detailed description of what is happening to $N(0)$ and $-\text{Im}\Sigma_{11}(0)$, in the presence of disorder, see Sec. VII of this paper, where we have analyzed their properties more closely and report, extensively, further numerical results.

V. LOCAL QUASI-PARTICLE DENSITY OF STATES CALCULATIONS

In this section we present results for the single site local quasi particle density of states calculations. As mentioned before we consider two types of disorder, (i) binary alloys where

we have two on-site potentials randomly distributed throughout the lattice and (ii) a uniform distribution of random on-site potentials. For both types of disorder we have solved, numerically, Eq. (9) in conjunction with its appropriate self-consistency conditions, for the order parameter, Δ , the average number density, n , and the self-energy, $\Sigma_{11}(i\omega_n)$.

The first situation we consider is a binary alloy of random on site energies ε_1 and ε_2 with equal concentration $c = 1 - c = 0.5$. The parameter we have chosen to use to describe the strength of the disorder is $\delta = \varepsilon_1 - \varepsilon_2$. Figure 5(a) shows the density of states in the normal state. The Van Hove singularity characteristic of a tight-binding model with nearest neighbor hopping on a square lattice is clearly visible for small disorder ($\delta = 0.6t$) in the middle of the band. As Fig. 5(a) shows, for more strongly disordered alloys this Van Hove peak is split into two peaks with some additional smearing. In the limit of δ being very large we get, as one would expect, band splitting of states associated with ε_1 and ε_2 respectively. On the other hand the disorder with uniform distribution of site energies, Fig. 6(a), gives only the smearing and flattening of density of states with, eventually, a complete flattening of the Van Hove peak.

The imaginary part of the self-energies for these two types of disorder are shown in Figs. 5(b) and 6(b) respectively. Evidently at low levels of disorder, they reflect the density of states of the clean system, and hence are consistent with the Born Approximation *via*. $-\text{Im}\Sigma_{11}(E) \propto N(E)$. For larger disorder strengths $\text{Im}\Sigma_{11}(E)$ is more flat for the uniform distribution, whereas for the binary alloy the self-energy is peaked not at the Van Hove singularity but at ε_1 and ε_2 .

Before turning to the problem of disordered d -wave superconductors for reference we have studied, briefly, the s -wave case. In short, we have introduced a site diagonal, local, attractive interaction with strength U , into the above model. As expected such interaction leads to conventional s -wave pairing. When implementing the CPA we have assumed that in this case the pairing order parameter Δ , which is now site diagonal does not vary from site to site. This is consistent with the Anderson theorem which was shown to be adequate for systems with a long coherence length.¹⁵ Fig. 7(a) shows the s -wave quasi-particle density

of states as calculated for various values of the binary alloy disorder strength δ . The results confirm that, for s -wave pairing, the gap is absolute and, whilst the edges may move, they remain well defined as required by Anderson's Theorem¹. In Fig. 7(b) we have also plotted the self-consistent self-energy as a function of the quasi-particle energy, for the same disorder strengths used to obtain Fig 7(a). From this graph we can see that $-\text{Im}\Sigma_{11}(E)$ is zero inside the gap and hence the normal disorder does not act as a pair breaker, for s -wave superconductivity.

The quasi-particle density of states for d -wave superconductors is dramatically different from the above BCS spectrum in the s -wave case even in the clean limit. As it is well known it has the characteristic v-like dip shown in Fig. 8(a), for ε near the chemical potential ($\mu = 0$). Upon introducing binary alloy disorder into the d -wave system one would naturally expect similarly different behavior from that described above and in Fig. 7. As is clear from the results reported in Fig. 8 this is indeed the case. Strikingly, as the analytic results of the previous section suggested, $N(0)$ becomes non-zero for the slightest disorder. This implies gapless superconductivity in contrast to the gaped one in the s -wave case.

In Fig. 8(b) we have plotted the self-energies, corresponding to the quasi-particle density of states results presented in Fig. 8(a). This shows a complex evolution with disorder, for small δ the imaginary part of the self-energy, $\Sigma(E)$, reflects the pure d -wave density of states (as expected in the SCBA limit) and hence $\text{Im}[\Sigma(0)] \sim 0$. However increasing δ leads to a finite $\Sigma(0)$, with a cusp like minimum in $\text{Im}[\Sigma(E)]$ at $E = 0$. Increasing the disorder even further, to $\delta = 2.8t$, the d -wave pairing is completely destroyed, and $\text{Im}\Sigma(E)$ reverts to the normal system self-energy. In this case $-\text{Im}\Sigma(E)$ is a maximum at $E = 0$, since the Fermi energy, $E_F = \mu$, was set exactly to 0.

VI. CRITICAL TEMPERATURE CALCULATIONS

To analyze the effect of the disorder upon T_c we have solved the gap equation together with the CPA equations. Again for the sake of comparison we have developed the analogous theory for the conventional s -wave superconductors based on the site diagonal particle-particle interaction, of strength U_0 , mentioned briefly in a previous sections. In this case neglecting the spatial fluctuations of Δ_i , and linearizing the gap equation for the configurationally averaged single site pairing potential $\bar{\Delta}$ we find the condition for the temperature T_c , below which $\bar{\Delta} \neq 0$, to be

$$1 = |U_0| \int_{-\infty}^{\infty} dE \frac{\bar{N}_i(E)}{2E} \tanh\left(\frac{\beta_c E}{2}\right) \quad (48)$$

where $\bar{N}_i(E)$ is the averaged density of states in the normal state at energy E , as calculated within the CPA, and $\beta_c = \frac{1}{k_B T_c}$.

The solution of Eq. (48) for T_c as a function of band filling and strengths of alloyed disorder, δ is shown in Fig. 9. From this figure we can see that the superconducting state exists for all band filling and the strength of disorder does little to suppress T_c . Again this is consistent with Anderson's theorem.

Now let us turn to the case where the interaction is non-local and the pairing potential Δ_{ij} connects nearest neighbors sites. Near T_c , where the gap equation is linear, the solutions can be labeled by their symmetries. Indeed we find two separate conditions on the temperature T_c for the instability of the normal state to d and extended s symmetry breaking. In the first case T_c^d is determined by

$$1 = -\frac{|U|}{4\pi} \frac{1}{N} \sum_{\vec{k}} \int_{-\infty}^{\infty} dE \operatorname{Im} \left(\frac{\eta_{\vec{k}}^2 G_{11}^c(\vec{k}; E)}{2E - \Sigma_{11}(E) - \Sigma_{22}(E)} \right) \tanh\left(\frac{\beta_c^d E}{2}\right) \quad (49)$$

and in the second extended s -wave case, T_c^s is given by

$$1 = -\frac{|U|}{4\pi} \frac{1}{N} \sum_{\vec{k}} \int_{-\infty}^{\infty} dE \operatorname{Im} \left(\frac{\gamma_{\vec{k}}^2 G_{11}^c(\vec{k}; E)}{2E - \Sigma_{11}(E) - \Sigma_{22}(E)} \right) \tanh\left(\frac{\beta_c^s E}{2}\right), \quad (50)$$

where $\eta_{\vec{k}}$ and $\gamma_{\vec{k}}$ refer to s -wave and d -wave like 'harmonics' defined previously following Eq. 19.

In Fig. 10 the critical temperature for both d -wave and extended s -wave pairing is shown as a function of band filling, n , for various strengths of alloyed disorder, δ . Full lines correspond to d -wave T_c while dashed ones to extended s -wave solutions. In the clean limit ($\delta = 0$) we can see that the extended s -wave solution exists mainly at the band edges and the d -wave solution is largely confined to the central portion of the band. For the interaction strength we have chosen, the two solutions cross at $n \approx 0.38$. Evidently for $n \leq 0.38$ the superconducting instability is at T_c^s whilst $n \geq 0.38$ the transition temperature is T_c^d . As we increase the strength of the alloyed disorder ($\delta/t = 0, 1.2, 2.0, 2.5, 2.6, 2.7, 2.8, 3.0$ from top to bottom curve) we see that both the T_c for the extended s -wave and d -wave solutions is reduced and for particularly strong disorder ($\delta = 2.7t$ and $\delta = 3.0t$) the maximum in the d -wave T_c is no longer at $n = 1$. This is connected with the splitting of Van Hove singularities visible in Fig. 5(a), *i.e.* the maximum in the normal-state density of states corresponds to the maximum in the d -wave T_c^d .

On the other hand for a uniform distribution of random site energies where there is no splitting of Van Hove singularities, and hence, we see a different tendency (Fig. 11, $\delta/t = 0, 1.0, 2.0, 3.0, 4.0, 5.0, 6.0$ from top to bottom curve). The maximum value of T_c^d is located at $n = 1$ no matter what the strength of disorder. For extended s -wave solutions and for relatively small disorder in the d -wave case the decreasing tendency in $T_c^{s,d}$ with growing disorder are very similar for the two types of disorder. However above a certain strength in either case we note that there is no crossing between the extended s -wave and d -wave solutions. This fact may be interpreted as the sign that the s and d states can not coexist or mix.

To compare the effect the two types of disorder have upon T_c we have, in Fig. 12, calculated T_c^d vs. δ/t at half filling for both binary alloy (solid line) and uniform (dashed line) disorder. From this graph we can see that the two types of disorder effect T_c in almost exactly the same manner. If we rescale the graphs such that the standard deviation in the disorder strength is the same, for uniform disorder $\sigma = \frac{\delta}{2\sqrt{3}}$ and for binary disorder $\sigma = \frac{\delta}{2}$, then the two curves lie very close to one another. This prompts the conclusion, which may

however be premature,⁵⁰ that T_c is not very sensitive to the details of the fluctuation in the site energy.

Other interesting point to investigate concerns the relative robustness of T_c against degradation by disorder in the cases of conventional s and d -wave pairing.³⁷ Fig. 13 shows the results for T_c for inter-site d -wave and on site s -wave superconductors versus alloyed disorder strength δ , where $n = 0.6$. Here one can easily recognize a typical difference between these two superconducting states. Clearly in case of a d -wave superconducting state disorder acts as an effective pair breaker while for s -wave superconductors it decreases T_c only slowly or not at all. An interesting physical consequence of this effect is that if both U_{ii} and U_{ij} ($i \neq j$) are attractive increasing disorder could lead to a transition from d -wave to s -wave pairing, as suggested by Abrikosov³⁷.

Evidently, the binary alloy disorder has certain features not shared by the uniform distribution of site energies model. One of these is the possibility of band splitting. For a very large δ parameter the band is split into two sub-bands, as shown in Fig. 14. The on site s -wave superconducting state is created within one of sub-bands. For disorder parameters: $c = 0.5$ and $\epsilon_1 = -\epsilon_2 = \delta/2$ we have not found any similar solution for d -wave, but for $c=0.25$ and $n=0.5$ a single sub-band d -wave solution is found. In Fig. 15 we show the very different behavior of T_c for a small and a large non-local interaction parameter, U_{ij} . For large enough U_{ij} the d -wave T_c does not go to zero when the band splits. The quasi-particle density of states corresponding to such a possibility is presented in Fig. 16 and, as in Fig. 14, we see the superconducting gap, which is now d -wave, has formed in one of the sub-bands.

To complete the discussion Figs. 17, 18 and 19 show the critical temperature plotted versus concentration c for various strength of binary alloy disorder δ with band fillings of $n = 1$ (Fig. 17), $n = 0.7$ (Fig. 18) and $n = 0.1$ (Fig. 19). Figs. 17 and 18 correspond to d -wave while Fig. 19 correspond to inter-site extended s -wave pairing. Again for large enough alloy disorder pair breaking phenomena take place. If disorder is introduced by a fixed potential δ , but varying the concentration of scatters, $c \ll 1$, from 0 we see that the results are similar to the case of a fixed c and increasing δ from 0. This shows that CPA

can work equally well, and indeed asymptotically exact, in both the Born (small δ) and T -matrix (small c) and resonant scattering regimes.

VII. $N(E)$ AND $\Sigma_{11}(E)$ AS $E \rightarrow 0$ AND THE LOW TEMPERATURE SPECIFIC HEAT

As mentioned earlier the behavior of the quasiparticle density of states $N(E)$ and the imaginary part of the self energy $\text{Im}\Sigma_{11}(E)$ near $E = 0$ is of general conceptual significance. For instance, the power law behavior of $N(E) \propto |E|^\alpha$, for d -wave superconductors give rise to power law dependence with temperature of many thermodynamic quantities, such as the specific heat $c_v(T)$, instead of the exponential cut-off characteristic of a gap in the quasiparticle spectrum.⁵ Naturally, dramatic changes in the low energy behavior of $N(\varepsilon)$ and $\text{Im}\Sigma_{11}(\varepsilon)$ as disorder is added to the problem is also of general interest and, as it turns out, of lively controversy.^{10-14,51,52} In this section we wish to examine those predictions of the CPA calculations which are relevant to these issues in particular. Using the methods outlined in the previous sections we calculate numerically the quasi-particle local density of states, $N(\varepsilon)$, and the self-energy, $\text{Im}\Sigma_{11}(\varepsilon)$, and then investigate how these two quantities change with both temperature and disorder.

For simplicity we have studied the half filled band ($\mu = 0$, $n = 1$). This is the band filling for which T_c , in the d -wave case, is a maximum. We will examine the effects of alloyed disorder on the system and show that as we increase the amount of scattering the specific heat vs. temperature relation changes from T^2 , in the clean limit, to T in the limit of strong scattering. As is widely recognized⁵ this behavior is the consequence of $N(E) \sim |E|$ changing to $N(E) = \text{constant}$ and is consistent with experiments.⁸

To get an impression of the form of $N(E)$ and $-\text{Im}\Sigma_{11}(E)$ in the region of the chemical potential, μ , we fit them to the function $a + b|E|^c$ in the energy range $-\Delta E < E < \Delta E$, where ΔE is small compared to the gap. Using the coefficients a , b and c to fit the curves $N(E)$ and $-\text{Im}\Sigma_{11}(E)$ in the region of μ gives us a tool to analyze their functional form.

For example a tells us if the curves are finite at $E = 0$, b controls the gradient of the curve and c controls the curvature.

In Figs. 20(a-c) we have plotted these coefficients, for $N(E)$, as a function of T , for different values of δ . We also included in Fig. 20(d) plots of the magnitude of the d -wave superconducting order parameter $|\Delta|$ vs. T , for the same values of alloyed disorder strength, δ , to indicate the temperature where the order parameter goes to zero. Regarding these curves as a brief summary of what the CPA predicts about the low energy behavior of $N(E)$ and $\Sigma(E)$ we now comment on their implications.

Firstly we note that in Fig. 20(a) the parameter $a(T)$ tends to a finite limit as $T \rightarrow 0$ and this limit increases more and more rapidly as the disorder described by δ , increases. Hence $N(0)$ is finite in agreement with our earlier discussion in Sec. IV where we derived for low scattering and low temperatures the dependence of $N(0)$ on δ (see Eq. (46)). It lends credit to the general consistency of our results that the $a(T) \cong N(0, T)$ curves rise to their normal state values as $T \rightarrow T_c$. Interestingly, as can be seen in Fig. 20(b) the gradient of $N(E)$, namely b , changes dramatically only near T_c . In fact for the case where δ is small (squares) the gradient even changes sign. This means that we go from having a gap in the density of states, below T_c to having a Van Hove singularity above T_c . The curvature, represented by c and plotted in Fig. 20(c), shows that for low disorder (squares) as we increase the temperature we go from a curvature of $c \leq 1$, ie. a cusp, to a curvature $c > 1$. Finally when the critical temperature is reached for each of the four different disorder types c goes to 2.

In the same manner, we now examine the corresponding coefficients, a' , b' and c' for $-\text{Im}\Sigma_{11}(E)$. In Figs. 21(a-c) we have plotted the calculated coefficients for $-\text{Im}\Sigma_{11}(E)$, at different values of δ as a function of the temperature. In Fig. 21(a) we can see that at low temperatures $-\text{Im}\Sigma_{11}(0)$ increases with disorder, again this agrees with our results in Sec. IV where an analytical form for the dependence of $-\text{Im}\Sigma_{11}(0)$ upon δ was derived at $T = 0$, see Eq. (47). As we increase the temperature we can see the self-energy at the chemical potential also rises until the normal state value is reached at the critical temperature. In Fig. 21(b) we can see how the gradient changes from being large for large δ and small for

small δ at low T , and at temperatures greater than T_c to be large and negative for large δ and small and negative for small δ . Finally Fig. 21(c) shows how, c , the curvature goes from being almost linear, $c = 1$, at low temperatures, regardless of δ , to $c = 2$ above T_c .

To illustrate the consequences of these results for the low temperature thermodynamic properties we have calculated the effect of disorder upon the specific heat. Using the above temperature dependent coefficients for the density of states near $\varepsilon \sim 0$ we calculated the limiting behavior of the specific heat as $T \rightarrow 0$. The results are shown in Fig. 22 for different strengths of disorder δ . In the case where δ is small (squares) we can see that the specific heat has a T^2 dependence (the plotted continuous solid line with no points) and for large δ the dependence upon temperature is linear, as expected.⁶

VIII. CONCLUSIONS

We have compared and contrasted the effect of disorder on conventional s - and d -wave superconductors on the bases of an extended, negative U Hubbard model and a mean field, CPA, treatment of disorder. On the one hand we have derived many of the well known results, such as the pair breaking formula in Eq. (34) or that for the quasi-particle density of states $N(0)$, Eq. (46). On the other hand we have solved the Gorkov-CPA equations Eqs. (14), (17) numerically and surveyed the salient features of their consequences by explicit calculations. The use of CPA in describing disordered d -wave superconductors is an advance in this very active field^{4-14,49,50} because it allows us to avoid the usually delicate choice between methods, sets of diagrams, designed to deal with either weakly or strongly scattering perturbations. The CPA treats both kinds of problems equally accurately and it is known to provide a very credible interpolation between the two⁴⁰. As an example where above feature of CPA may have a crucial role to play we recall the use of the resonant scatterer model in interpreting experimental data both on the cuprates^{8,53} and some Heavy Fermion systems.^{11,54} In short, note that in the impurity, $c \rightarrow 0$, limit the self energy for the Greens function describing an electron moving on a lattice, is given by

$$\Sigma(E) = cT(0, 0; E), \quad (51)$$

where the T -matrix is defined, in terms of the impurity ‘potential’ V_{imp} , a real local shift in the site energy, as

$$T(0, 0; E) = \frac{V_{imp}}{1 - V_{imp}G(0, 0; E)}. \quad (52)$$

Evidently $T(0, 0; \epsilon)$ is complex number with an amplitude:

$$a(E) = \sqrt{(1 - V_{imp}\text{Re}G(0, 0; E))^2 + (V_{imp}\text{Im}G(0, 0; E))^2}$$

and a phase, the phase shift $\phi(E)$, given by

$$\tan \phi(E) = \frac{V_{imp}\text{Im}G(0, 0; E)}{1 - V_{imp}\text{Re}G(0, 0; E)}. \quad (53)$$

Now, observe that while for weak scatterers

$$\text{Im}\Sigma^B(E) = -c\pi |V_{imp}|^2 N(E) \quad (54)$$

for a resonant scatterer in the unitary limit, defined by $\phi(E) = \frac{\pi}{2}$,

$$\text{Im}\Sigma^R(E) = -c\frac{\pi}{N(E)}, \quad (55)$$

where $N(E) = -\frac{2}{\pi}\text{Im}G(0, 0; E)$. It is the above dramatic difference in the dependence of $\text{Im}\Sigma^B$ and $\text{Im}\Sigma^R$ on the density of states $N(E)$ that the cited authors rely on in interpreting the relevant experimental data. Evidently, since the individual scattering events described by the local T -matrices are always treated exactly in the CPA, the CPA describes weak scatterers and resonant scatterers equally well. Moreover, since it is a reliable approximation not only in the impurity limit, $c \sim 0$, but also for arbitrary concentrations it deals with resonance scatterers even when Eq. (55) no longer holds. Thus CPA should be the preferred treatment for models with strong, even resonant scattering.

Although we have not specifically concentrated on this aspect of the method, the principle feature of Eqs. (54) and (55), namely the dependence of $\Sigma(E)$ on $N(E)$, can be seen to be

at work in our calculations of the previous section. To demonstrate this we have calculated $\Sigma(0)$ and $N(0)$ as functions of band filling, n , in the most interesting region $n \sim 1.0$, and compared in Fig. 23 their relationships for weak and strong scatterers at $c = 0.5$. Clearly, for weak scatterers $\delta/t = 1$, $-\text{Im}\Sigma(0)$ is a more or less linear function of $N(0)$ as in Eq. (54), while for strong scatterers $\delta/t = 3$, $\text{Im}\Sigma(0)$ is inversely proportional to $N(0)$ as in the resonant scatterers model described by Eq. (55). Thus we conclude that the CPA employed in the calculation gives a reliable account of disorder in both the weak and strong scattering regimes.

Having listed the above desirable properties of the CPA we hasten to emphasize that it is a ‘mean–field’ theory of disorder and, hence, does not describe such interesting phenomena as localization⁵³ even in the normal state.⁵⁴ Consequently, our result that $N(0)$ is finite for the smallest amount of disorder can not be taken as evidence against the conclusion that $N(E) \sim |E|^\alpha$ of Nersesyan *et al.*¹⁴ As this originates from the divergence of the vertex corrections in perturbation series for $\Sigma(E)$ we may conjecture that it has to do with localization effects not described by CPA. This very interesting point is in the need of further clarification, and indeed we shall return to it in a later publication.

ACKNOWLEDGMENTS

This work has been partially supported by EPSRC under grant number GR/L22454 and KBN grants 2P 03B 031 11 and 2P 03B 050 15. A.M. Martin would also like to thank the TMR network Dynamics of Nanostructures.

APPENDIX A: THE RECURSION METHOD FOR CPA

The recursion method⁵⁵ was first used for solving the Bogoliubov de Gennes Equation by Annett and Goldenfeld⁵⁶ and Litak *et al.*⁵⁷. Its use to implement CPA calculations was advocated by Julien and Mayo⁵⁸. Here, as in reference,⁴⁸ we made a combined use of these powerful methods to calculate the Greens function matrix

$$G_{\alpha\alpha'}^c(i, j; E) = \langle i\alpha | \frac{1}{E\mathbf{1} - \mathbf{H}} | j\alpha' \rangle \quad (\text{A1})$$

where the indices i and j denote sites, while α and α' represent the particle or hole degree of freedom on each site. We denote particle degrees of freedom by $\alpha = 1$ and hole degrees of freedom by $\alpha = 2$. For example $G_{12}^c(i, j; E)$ represents the Greens function between the particle degree of freedom on site i and the hole degree of freedom on site j at energy E .

To compute the Greens functions (A1) we can closely follow the method described by Martin and Annett.⁴⁸ Using this method we can transform the Hamiltonian to a block tridiagonal form

$$E\mathbf{1} - \mathbf{H} = \begin{pmatrix} E\mathbf{1} - \mathbf{a}_0 & -\mathbf{b}_1 & 0 & 0 & 0 & 0 & 0 & \cdots \\ -\mathbf{b}_1^\dagger & E\mathbf{1} - \mathbf{a}_1 & -\mathbf{b}_2 & 0 & 0 & 0 & 0 & \cdots \\ 0 & -\mathbf{b}_2^\dagger & \ddots & \ddots & 0 & 0 & 0 & \cdots \\ 0 & 0 & \ddots & \ddots & \ddots & 0 & 0 & \cdots \\ 0 & 0 & 0 & -\mathbf{b}_n^\dagger & E\mathbf{1} - \mathbf{a}_n & -\mathbf{b}_{n+1} & 0 & \cdots \\ \vdots & \vdots & \vdots & 0 & \ddots & \ddots & \ddots & \ddots \end{pmatrix} \quad (\text{A2})$$

where \mathbf{a}_n and \mathbf{b}_n are 2×2 matrices. Given this form for $\langle i\alpha | E\mathbf{1} - \mathbf{H} | j\alpha' \rangle$ and expressing the Greens function as

$$G_{\alpha\alpha'}^c(i, j; E) = \langle i\alpha | (E\mathbf{1} - \mathbf{H})^{-1} | j\alpha' \rangle, \quad (\text{A3})$$

the Greens functions above can be evaluated as a matrix continued fraction so that

$$\mathbf{G}(i, j; E) = \left(E\mathbf{1} - \mathbf{a}_0 - \mathbf{b}_1^\dagger \left(E\mathbf{1} - \mathbf{a}_1 - \mathbf{b}_2^\dagger \left(E\mathbf{1} - \mathbf{a}_2 - \mathbf{b}_3^\dagger (E\mathbf{1} - \mathbf{a}_3 - \dots)^{-1} \mathbf{b}_3 \right)^{-1} \mathbf{b}_2 \right)^{-1} \mathbf{b}_1 \right)^{-1} \quad (\text{A4})$$

where

$$\mathbf{G}^c(i, j; E) = \begin{pmatrix} G_{\alpha\alpha}^c(i, i; E) & G_{\alpha\alpha'}^c(i, j; E) \\ G_{\alpha'\alpha}^c(j, i; E) & G_{\alpha'\alpha'}^c(j, j; E) \end{pmatrix}. \quad (\text{A5})$$

Within Eqs. (A2) and (A4) we have a formally exact representation of the Greens functions. However in general both the tridiagonal representation of the Hamiltonian, and

the matrix continued fraction (A2) will be infinite. In practice one can only calculate a finite number of terms in the continued fraction exactly. In the terminology of the recursion method it is necessary to *terminate* the continued fraction.^{55,57,59–63}

If we were to calculate up to and including \mathbf{a}_n and \mathbf{b}_n and then simply set subsequent coefficients to zero then the Greens function would have $2n$ poles along the real axis. The density of states would then correspond to a set of $2n$ delta functions. In order to obtain accurate results it would be necessary to calculate a large number of exact levels, which would be expensive in terms of both computer time and memory.

As a more efficient alternative we choose to terminate the continued fraction using the extrapolation method, as used previously by Litak, Miller and Györfy.⁵⁷ We calculate the values for \mathbf{a}_n and \mathbf{b}_n exactly up to the first m coefficients using the recursion method. Then, noting the fact that the elements of the matrices \mathbf{a}_n and \mathbf{b}_n vary in a predictable manner,⁵⁷ we extrapolate the elements of the matrices for a further k iterations, where k is usually very much greater than m . This enables us to compute the various Greens functions accurately with relatively little computer time and memory.

We now have a method for calculating the Greens Function $G_{\alpha\alpha'}^c(i, j; E)$. To calculate our system of equations self-consistently for a given site i , we need to know $G_{12}^c(i, j_1; E)$, $G_{12}^c(i, j_2; E)$, $G_{12}^c(i, j_3; E)$ and $G_{12}^c(i, j_4; E)$. If the interaction is non-local, else if the interaction is local then we only need to calculate $G_{12}^c(i, i; E)$, see Fig. 1. To calculate \bar{n} we also need $G_{11}^c(i, i; E)$.

In performing our self-consistency calculation we can make use of the fact that $\Sigma(E)$ just acts as a renormalization to $E \mapsto \tilde{E}$ (see Sec. IV). This means we do not need to recalculate \mathbf{a}_n and \mathbf{b}_n when we calculate the self-consistent self-energy. We first calculate the order parameter self-consistently for a given attractive interaction, then we calculate $\mathbf{G}^c(i, i; E)$ and hence the self-energy self-consistently (remembering that in this self-consistent loop we do not need to recalculate \mathbf{a}_n and \mathbf{b}_n , since the self-energy does not affect them). Then we recalculate the superconducting order parameter self-consistently, incorporating the calculated self energy and repeat this procedure until both the order parameter and the self

energy have reached stable self-consistent solutions.

REFERENCES

- ¹ P.W. Anderson, J. Phys. Chem. Solids **11**, 26 (1959).
- ² A.A. Abrikosov and L.P. Gorkov, Sov. Phys. JETP **8**, 1090 (1959); *ibid.* **9**, 220 (1959).
- ³ L.P. Gorkov, Sov. Sci. Rev. A. Phys. **9**, 1 (1987).
- ⁴ W.N. Hardy, D.A. Bonn, D.C. Morgan, R.X. Laing and K. Zhang, Phys. Rev. Lett. **70**, 3999 (1993); D.A. Bonn, S. Kammal, K. Zhang, R.X. Liang, D.J. Baar, E. Klein and W.N. Hardy, Phys. Rev. B **50**, 4051 (1994).
- ⁵ J.F. Annett, N. Goldenfeld and A.J. Leggett in “Physical Properties of High Temperature Superconductors”, Vol. 5, D.M. Ginsberg (ed.), (World Scientific, Singapore 1996).
- ⁶ F. Gross, B.S. Chandrasekhar, D. Einzel, K. Andres, P.J. Hirschfeld, H.R. Ott, J. Beuers, Z. Fisk and J.I. Smith, Z. Phys. B **64**, 175 (1986).
- ⁷ K. Maki in “Superconductivity”, Parks (Ed.) (1969) Vol. 2, Chapter 8.
- ⁸ P.J. Hirschfeld and N.D. Goldenfeld, Phys. Rev. B **48**, 4219 (1993).
- ⁹ M. Prohammer and J.P. Carbotte, Phys. Rev. B **43**, 5370 (1991).
- ¹⁰ L.P. Gorkov and P.A. Kalugin JETP Lett. **41**, 253 (1983).
- ¹¹ S. Schmitt-Rink, K. Miyake and C.M. Varma, Phys. Rev. Lett. **57**, 2575 (1986).
- ¹² P.A. Lee, Phys. Rev. Lett. **71**, 1887 (1993).
- ¹³ A.V. Balatsky and M.I. Salkola, Phys. Rev. Lett. **76**, 2386 (1996).
- ¹⁴ A.A. Nersisyan, A.M. Tsvetik and F. Wenger, Phys. Rev. Lett. **72**, 2628 (1994), A.A. Nersisyan, A.M. Tsvetik and F. Wenger, Nuc. Phys. B **438**, 561 (1995), A.A. Nersisyan and A.M. Tsvetik, Phys. Rev. Lett. **78**, 3981 (1997).
- ¹⁵ B.L. Gyorffy, G. Litak and K.I. Wysokiński, in M. Ausloos, A.A. Varlamov (Eds.) *Fluctuation Phenomena in High Temperature Superconductors*, NATO ASI Series, 1997.

- ¹⁶ K. Westerholt and B. Von Hedt, J. Low Temp. Phys. **95**, 123 (1994).
- ¹⁷ A.I. Larkin, JETP Lett. **2**, 130 (1965).
- ¹⁸ N. Peng and W.Y. Liang, Physica C **233**, 61 (1994).
- ¹⁹ K. Uchinokura, T. Ino, I. Terasaki and I. Tsukada, Physica B, **205**, 234 (1995).
- ²⁰ E.R. Ulm, J.T. Kim, T.R. Lemberger, S.R. Foltyn and X.D. Wu, Phys. Rev. B **51**, 9193 (1995).
- ²¹ Gang Xiao *et al.* Phys. Rev. B **43**, 1245 (1990).
- ²² C. Bernhard, J.L. Tallon, C. Bucci, R. De Renzi, G. Guidi, G.V.M. Williams and Ch. Niedermayer, Phys. Rev. Lett. **77**, 2304 (1996).
- ²³ Y.K. Kuo *et al.*, Phys. Rev. **B56**, 6201 (1997).
- ²⁴ G.V.M. Williams and J. T. Tallon, Phys. Rev. **B57**, 10 984 (1998).
- ²⁵ J. Giapintzakis, D.M. Ginsberg, M.A. Kirk and S. Ockers, Phys. Rev. B **50**, 15967 (1994).
- ²⁶ V.F. Elesin, K.E. Kon'kov, A.V. Krashennnikov and L.A. Openov, Sov. phys. JETP **83**, 395 (1996) [Zh. Eksp. Teor. Fiz. **110**, 731 (1996)].
- ²⁷ K.Karpińska *et al.*, Mol. Phys. Reports **20**, 91 (1997).
- ²⁸ S.Haas, A.V. Balatsky, M. Sigrist and T.M. Rice, Phys. Rev. **B56**, 5108 (1997).
- ²⁹ A.P. Kampf and T.P. Devereaux, Phys. Rev. **B56**, 2360 (1997).
- ³⁰ G. Harań and A.D. Nagi, Phys. Rev. **B58**, 12 441 (1998).
- ³¹ B.C. den Hertog and M.P. Das, Phys. Rev. **B58**, 2838 (1998).
- ³² R.J. Radtke, K.Levin, H.-B. Schüttler and M.R. Norman, Phys. Rev. B **48**, 653 (1993).
- ³³ L.A. Openov, Pis'ma Zh. Eksp. Teor. Fiz. **66**, 627 (1997) [JETP Lett. **66**, 661 (1997)].

- ³⁴ J.M. Byers, M.E. Flatte and D.J. Scalpino, Phys. Rev. Lett. **71**, 3363 (1993); M.E. Flatte and J.M. Byers, *ibid.* **78**, 3761 (1997).
- ³⁵ W. Xu, W. Kim, Y. Ren and C.S. Ting, Phys. Rev. B **54**, R12693 (1996).
- ³⁶ T. Xiang and J.M. Wheatley, Phys. Rev. B **51**, 11721 (1995).
- ³⁷ A.A. Abrikosov, Physica C **244**, 243 (1995).
- ³⁸ H.A. Blackstead and J.D. Dow, Phys. Lett. A **206**, 107 (1995). M.B. Maple, M.J. Kramer and R.W. McCallum, *ibid.* **206**, 111 (1995).
- ³⁹ H. Hasegawa, Supplement to Prog. Theor. Phys. **53**, 139 (1973).
- ⁴⁰ R.J. Elliot, J.A. Krumhansl and P.L. Leath, Rev. Mod. Phys. **46**, 465 (1974).
- ⁴¹ R. Vlaming and D. Vollhardt, Phys. Rev. B **45**, 4637 (1992).
- ⁴² H. Lustfeld, J. Low Temp. Phys. **12**, 595 (1973); G. Kerker and K.H. Bennemann, Solid State Commun. **14**, 365 (1974); K.I. Wysokiński and A.L. Kuzemsky, J. Low Temp. Phys. **52**, 81 (1983).
- ⁴³ G. Litak, K.I. Wysokiński, R. Micnas, St. Robaszkiewicz, Physica C **199**, 191 (1992)
- ⁴⁴ G. Litak, A.M. Martin, B.L. Györfy, J.F. Annett and K.I. Wysokiński, Physica C to be published.
- ⁴⁵ F. Wenger, Z. Phys. B **98**, 171 (1995).
- ⁴⁶ M. Tinkham, Introduction to Superconductivity (McGraw-Hill, New York, 1975).
- ⁴⁷ R.M. Dreizler and E.K.U. Gross, Density Functional Theory (Springer, Berlin, 1990).
- ⁴⁸ A.M. Martin and J.F. Annett, Phys. Rev. B **57**, 8709 (1998).
- ⁴⁹ R. Fehrenbacher, Phys. Rev. Lett. **77**, 1849 (1996).
- ⁵⁰ S.V. Pokrovsky, V.L. Pokrovsky, Phys. Rev. B **54**, 13275 (1996).

- ⁵¹ K.Ziegler, M.H. Hettler and P.J. Hirschfeld, Phys. Rev. Lett. **77**, 3013 (1996).
- ⁵² A.A. Nersesyan and A.M. Tsvelik, Phys. Rev. Lett. **78**, 3981 (1997).
- ⁵³ B. Kramer and A. MacKinnon, Rep. Prog. Phys. **56** 1469 (1993).
- ⁵⁴ A.M. Goldman and N. Marković, Physics Today, November 1998 pp. 39.
- ⁵⁵ R. Haydock, in: Solid state Physics, Vol. **35**, eds. Ehrenreich, F. Seitz and D. Turnbull (Academic Press, New York, 1980).
- ⁵⁶ J.F. Annett and N. Goldenfeld, J. Low. Temp. Phys. **89**, 197 (1992).
- ⁵⁷ G. Litak, P. Miller and B.L. Györfy, Physica C **251**, 263 (1995).
- ⁵⁸ J.P. Julien and D. Mayo, J. Phys F **3**, 1861 (1993).
- ⁵⁹ A. Magnus in: Solid State Sciences **58** eds. D.G. Pettifor and D.L. Weaire (Springer 1984).
- ⁶⁰ F. Ducastelle, P. Turchi and G. Tréglia in: Solid State Sciences **58** eds. D.G. Pettifor and D.L. Weaire.
- ⁶¹ C.M.M. Nex in: Solid State Sciences **58** eds. D.G. Pettifor and D.L. Weaire (Springer 1984).
- ⁶² G. Allan in: Solid State Sciences **58** eds. D.G. Pettifor and D.L. Weaire (Springer 1984).
- ⁶³ A. Trias, M. Kiwi and M. Weissmann, Phys. Rev. B **28**, 1859 (1983).

FIGURES

FIG. 1. Schematic diagram of a tight binding lattice with particle and hole degrees of freedom. The gap parameter Δ_{ij} couples particles on site i to holes on site j . The difference between local and non-local pairing is highlighted by the dashed (local pairing) and solid (non-local pairing) lines.

FIG. 2. The effective pair-breaker ρ_c as calculated (i) by numerically finding $\frac{T_c}{T_{c0}}$ and inverting Eq. (36) (squares), (ii) numerically finding $\text{Im}\Sigma_0$ and using this in Eq. (37) (solid line) and (iii) Using the self-consistent Born approximation to find $\text{Im}\Sigma_0$ and then evaluating Eq. (37) (dashed line).

FIG. 3. A comparison of the density of states at the chemical potential vs. different strengths of alloyed disorder δ/t . The solid line is the analytical form derived in Eq. (48) and the dashed one represent are our self-consistent numerical calculations.

FIG. 4. A comparison of the density of states at the Fermi energy vs. different strengths of disorder with a uniform distribution between $-\frac{\delta}{2}$ and $\frac{\delta}{2}$. The solid line is the analytical form derived in Eq. (48) and the dashed one represent our numerical calculations.

FIG. 5. (a) Density of states $N(E)$ and, (b), self-energies $\text{Im}\Sigma(E)$ for a normal state with various alloyed disorder strengths δ/t , calculated for a local interaction $|U| = 3.5t$ and $n = 1$.

FIG. 6. (a) Density of states $N(E)$ and (b) self-energies $\text{Im}\Sigma(E)$ for a normal state with various uniform disorder strengths δ/t , calculated for a local interaction $|U| = 3.5t$ and $n = 1$.

FIG. 7. (a) Density of states $N(E)$ and (b) self-energies $\text{Im}\Sigma(E)$ for a superconducting state with various alloyed disorder strengths δ/t , calculated for a local interaction $|U| = 3.5t$ and $n = 1$.

FIG. 8. (a) Density of states $N(E)$ and (b) self-energies $\text{Im}\Sigma(E)$ for a superconducting state with various uniform disorder strengths δ/t , calculated for a non-local interaction $|U| = 3.5t$ and $n = 1$.

FIG. 9. Critical temperature T_c vs. band filling n for a local s -wave superconductor with various alloyed disorder strengths δ/t , calculated for a local interaction $|U| = 3.5t$.

FIG. 10. Critical temperature for d -wave and extended s -wave order parameters as function of band filling for different strengths of alloyed disorder δ/t , calculated for a non-local interaction $|U| = 3.5t$.

FIG. 11. Critical temperature for d -wave and extended s -wave order parameters as a function of band filling for different strengths of uniform disorder δ/t , calculated for a non-local interaction $|U| = 3.5t$.

FIG. 12. Critical temperature of the d -wave superconducting state vs. the strength of disorder. The solid line is for a uniform distribution of disorder and the dashed line is for a binary alloy, where $c = 0.5$ and in both cases $n = 1$ and the non-local interaction $|U| = 3.5t$.

FIG. 13. Critical temperature of d -wave (solid line) and local s -wave (dashed line) superconducting pairing states as a function of alloyed disorder for $|U| = 3.5t$, $n = 0.6$ and $c = 0.5$.

FIG. 14. Local density of states, at zero temperature, for an alloyed disorder of $\delta/t = 6$, a local interaction $|U| = 3.5t$, $n = 0.6$ and $c = 0.5$.

FIG. 15. Critical temperature of the d -wave superconducting state as a function of alloyed disorder strength shown for different interaction strengths, $c = 0.25$ and $n = 0.5$.

FIG. 16. Local particle density of states, for an alloyed disorder of $\delta/t = 8$, a non-local interaction $|U| = 3.5t$, $n = 0.5$ and $c = 0.25$.

FIG. 17. Critical temperature vs. concentration, at different alloyed disorder strengths, for a non-local interaction $|U| = 3.5t$ and $n = 1.0$.

FIG. 18. Critical temperature vs. concentration, at different alloyed disorder strengths, for a non-local interaction $|U| = 3.5t$ and $n = 0.7$.

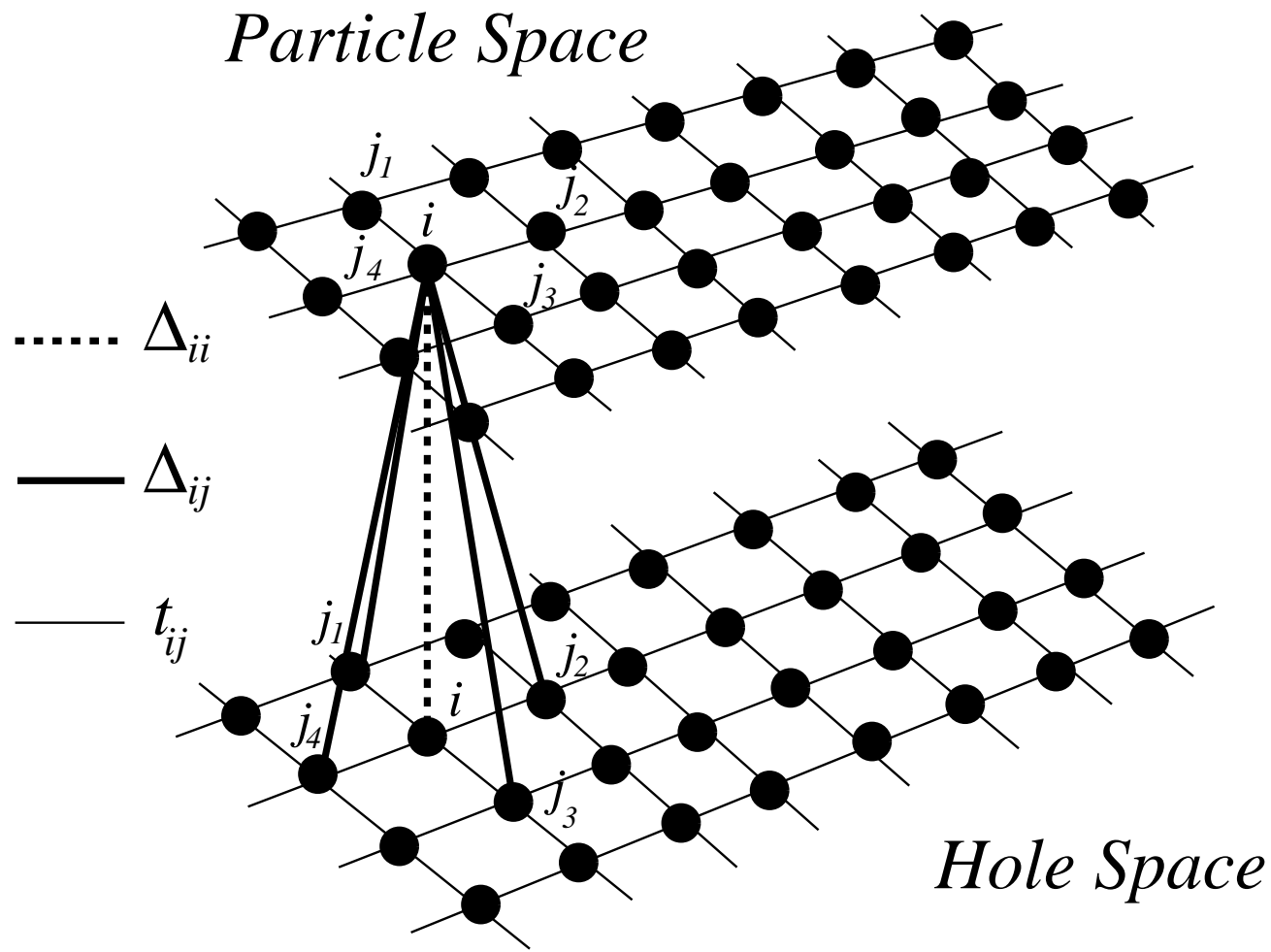
FIG. 19. Critical temperature vs. concentration, at different alloyed disorder strengths, for a non-local interaction $|U| = 3.5t$ and $n = 0.1$.

FIG. 20. The coefficients a (a), b (b) and c (c) which represent the Local Particle Density of States in the region of the chemical potential as a function of temperature, for different alloyed disorder strengths δ ($\delta = 0.6t$ (diamonds), $\delta = 1.0t$ (+), $\delta = 2.0$ (squares) and $\delta = 2.6t$ (\times)). In (d) we have also plotted the magnitude of the d -wave gap vs. temperature, for the same alloyed disorder strengths as in figures (a), (b) and (c). In all four figures the interaction is non-local with $|U| = 3.5t$, $n = 1$ and $c = 0.5$.

FIG. 21. The coefficients a' (a), b' (b) and c' (c) which represent the imaginary part of the self-energy, in the region of the Fermi energy, as a function of temperature, for different alloyed disorder strengths δ ($\delta = 0.6t$ (diamonds), $\delta = 1.0t$ (+), $\delta = 2.0t$ (squares) and $\delta = 2.6t$ (\times)). The interaction is non-local with $|U| = 3.5t$, $n = 1$ and $c = 0.5$.

FIG. 22. The specific heat as a function of temperature for different strengths of alloyed disorder δ ($\delta = 0.6t$ (squares), $\delta = 1.0t$ (circles), $\delta = 2.0t$ (triangles) and $\delta = 2.6t$ (+)), again the interaction is non-local with $|U| = 3.5t$, $n = 1$ and $c = 0.5$.

FIG. 23. Relations between $\text{Im}\Sigma(0)$ and $N(0)$ for weak $\delta/t = 1.0$ and strong $\delta/t = 3.0$ scatterers in binary alloys ($c = 0.5$).



Particle Space

Hole Space

